EPRI

A Positive Sequence Model for Aggregated Representation Electric Vehicle Chargers

EPCL Model Description

EPRI Project 1-116982

A Positive Sequence Model for Aggregated Representation Electric Vehicle Chargers

EPCL Model Description

EPRI Project 1-116982

November 2022

Lead Engineer: L. Sundaresh
Project Manager: P. Mitra

DISCLAIMER OF WARRANTIES AND LIMITATION OF LIABILITIES

Together…Shaping the Future of Energy®

CONTENTS

LIST OF FIGURES

LIST OF TABLES

1
POSITIVE SEQUENCE MODEL OF EV CHARGERS

Introduction

Over the next few years, rate of Electric Vehicles (EVs) sales is predicted to rapidly increase. As a result, EV chargers are going to be a considerable portion of the electrical load [1,2] and their aggregate response is expected to have a significant impact on the stability of the bulk electric system. Therefore, there is a need to model their aggregate behavior accurately and incorporate them in the bulk power system dynamic studies. In this report, a positive sequence model that captures the aggregate behavior of the EV chargers is developed.

The impact of increased EV charger model on bulk electric system has recently started to receive attention. Six different EV chargers were tested under different voltage sag conditions and a simplified model for these chargers was developed in [3]. Based on this work, EV charger models were used in a distribution level feeder study described in [4] to study the impact of increased adoption of EV chargers on the delayed voltage recovery observed in the feeder. The active power response of the six different EV charger characteristics reported in [3, 4] are shown in Fig. 1. The positive sequence model developed in this work is based on the responses observed and documented in [3,4], and is intended to capture the aggregated response of different proportions of these chargers connected to a distribution system at the substation head. The ultimate objective is to use the positive sequence model developed here for a system-wide study in a transmission planning tool to identify the system wide impacts of having a significant amount of EV charging loads on the grid.

For the purposes of development of this aggregated positive sequence model, the responses of the six types of EV chargers, were categorized under 3 different categories:

1. EV-A, EV-C, and EV-E has a small dip in the active power consumption following the fault and promptly returns to its normal operation level within 0.2s. For the purposes of aggregated modeling, this dip was neglected, and the EV chargers are assumed to have a constant power operation.

2. For (EV-D), the power consumed by the EV charger decreased during the fault and reduced to zero after a time delay. It then ramped up to the pre-fault levels after a time delay.

3. For EV-B and EV-F the active power consumption dropped at the beginning of the fault and the power drawn remained zero for a set amount of time before ramping up back to the pre fault levels. The duration of the cessation and the ramp rate varied between the charger models.

The model described in the next section has been developed to capture the aggregate response at the substation head of having user defined proportions of these 3 different categories of EV chargers in the distribution feeder. The model has been developed for the GE-PSLF™ simulator in their EPCL programming language.

It is worthwhile to mention that at this stage no information was available on the reactive power consumption of these EV chargers from the reports published earlier [3, 4]. As such, it is assumed that the reactive power consumption may have a dynamic behavior similar to the active power consumption shown in Fig. 1. However, this topic can be revisited as more relevant data becomes available.

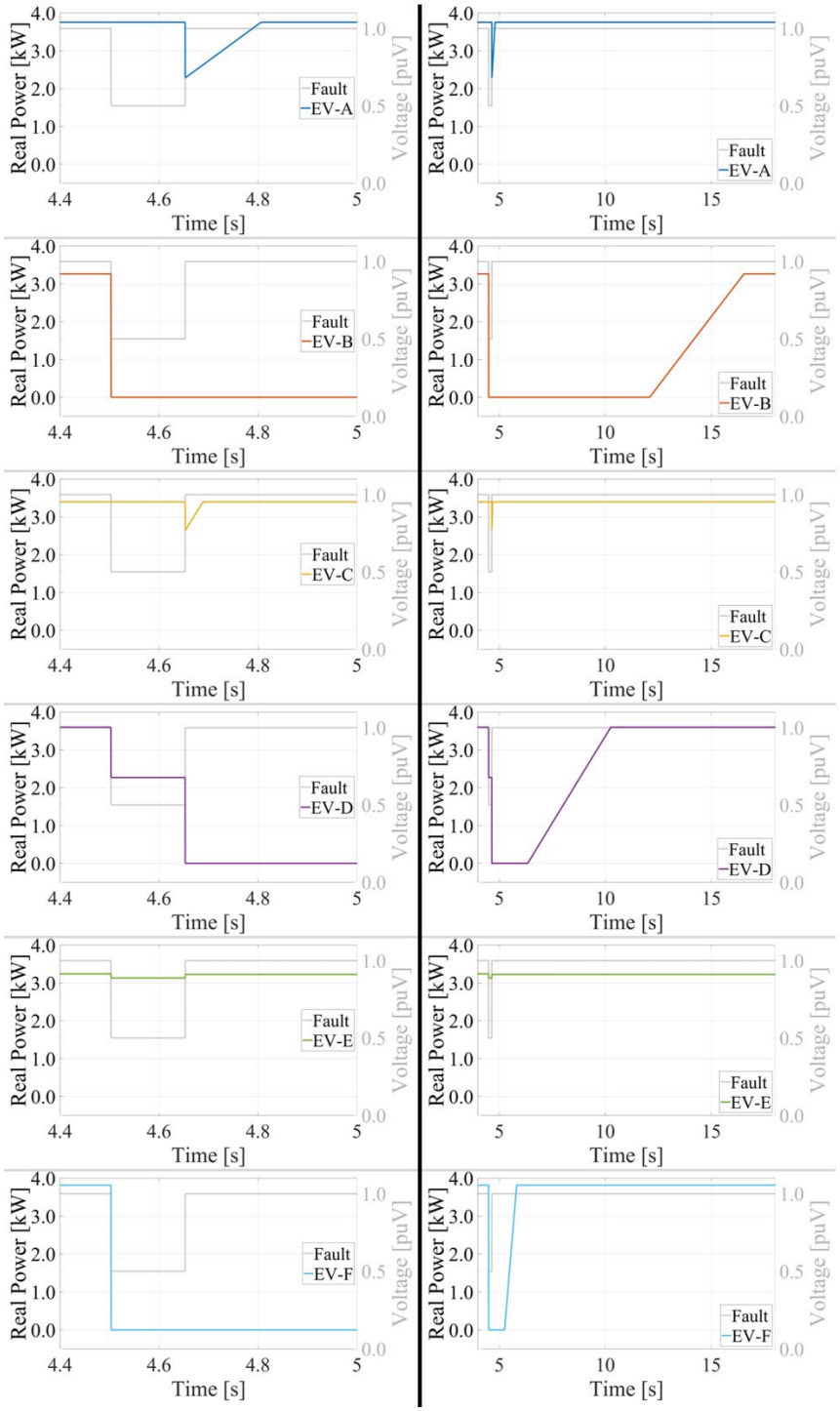

Figure 1 Summary of the different EV charger responses for a voltage sag [4]

Model description

A detailed description of the proposed EV charger model is presented in this section. The active power and reactive power output of the EV charger model can be tuned independently. As mentioned in the previous section, the structures of the active and reactive power response paths are similar. The only difference being the inclusion of an optional frequency-based droop for active power output of the load. The block diagrams for the active and reactive power consumption of this proposed model are shown in Fig. 2 and Fig 3 respectively.

The initial value of the active and reactive power input into the block P_0 and Q_0 are taken from the power flow solution during the initialization of the model.

Brief descriptions of each of the control blocks are as follows:

1. The voltage magnitude at the terminal of the model (Vt) is measured at each time step and passed through a washout block. The washout block can be deactivated as needed by setting the value of T_{vp} to 0.
2. An optional frequency based active power droop logic is also included in this model. This can be activated or deactivated by setting a suitable value of the droop gain K_{droop}
3. A lead lag compensator is included to adjust the transient response of the model.
4. This model represents the aggregate response of different types of EV chargers at a feeder/ substation level. To account for the different responses of individual EV chargers in an aggregated model, the model allows the user to specify different fractions (FrA, FrB, FrC) to simulate different characteristics as described in the previous section. The different characteristics can be created by parameterizing the control logic (described in bullet 7) appropriately.
5. The parameters nPA/nQa, nPB/nQB, nPC/nQC, and nPD/nQD of each fraction are used to specify the dependence of active and reactive power consumption of the load with voltage variations as constant power, constant current, or constant impedance.
6. Block 6 converts the active/reactive power to a current quantity that can compared against the limits.
7. Current limiters are included for each of these fractions to ensure that the current consumption does not exceed a specified value even with a constant power behavior. Also note that a load convention has been used for this model, which means that a positive value of current means the device consuming current and a negative value implies that the device is injecting current.
8. The control logic ensures that if the voltage drops below V_{cease} for T_{cease} s, the respective fraction (F_{cease}) of the EV charger load ceases to consume active power after a delay of T_{delay} s. The T_{delay} s term has been added to emulate the delay that EV chargers may have before they cease to charge. If the voltage recovers above $V_{reconnect}$ for $T_{reconnect}$ seconds, the active power consumption is ramped to the nominal value in T_{ramp} seconds.
9. The last transfer function with a time constant of T_{num} has been included to ensure numerical stability. The value of T_{num} is hardcoded to 4*delt. Hence, if a user chose a simulation time step of 0.0042s this time constant is automatically set to 0.0168s.

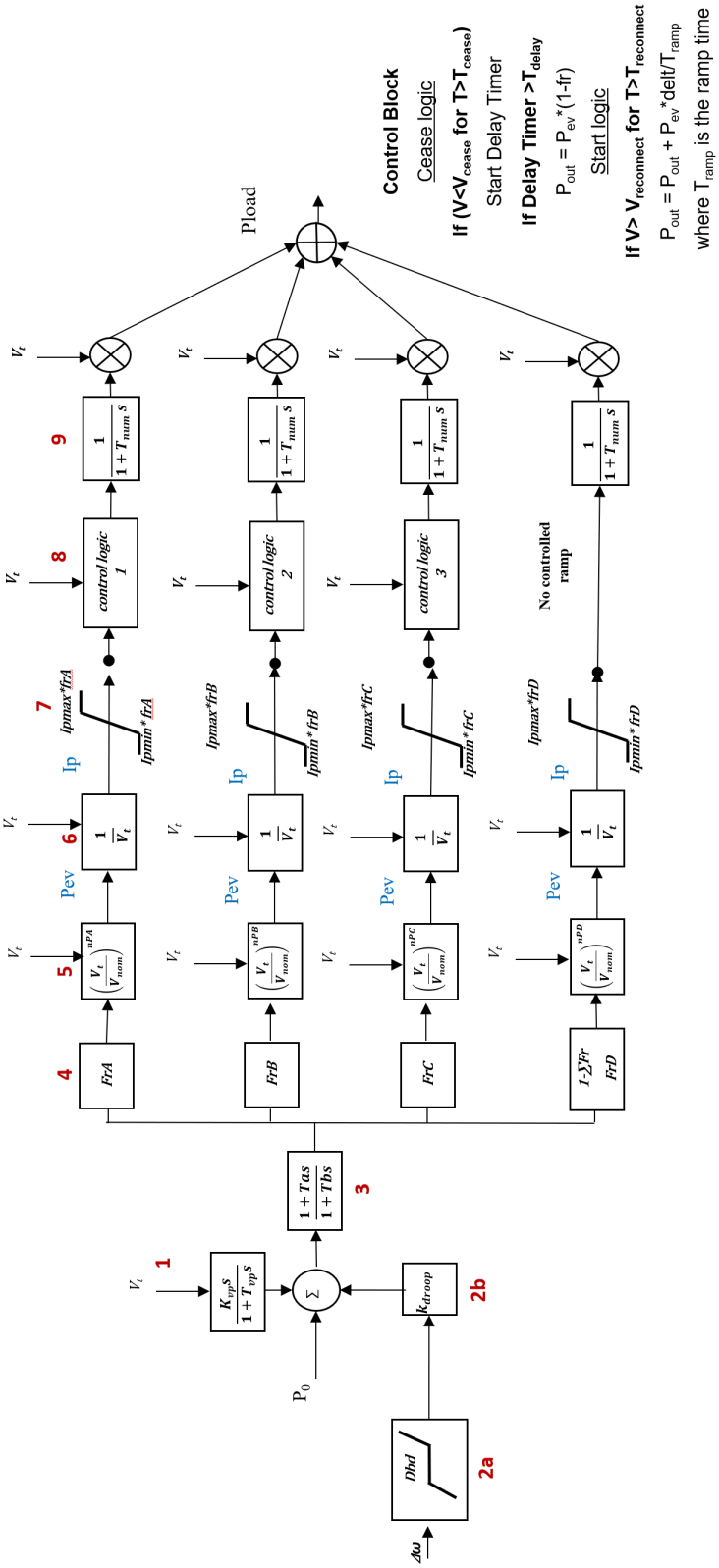

Figure 2 Active power control loop

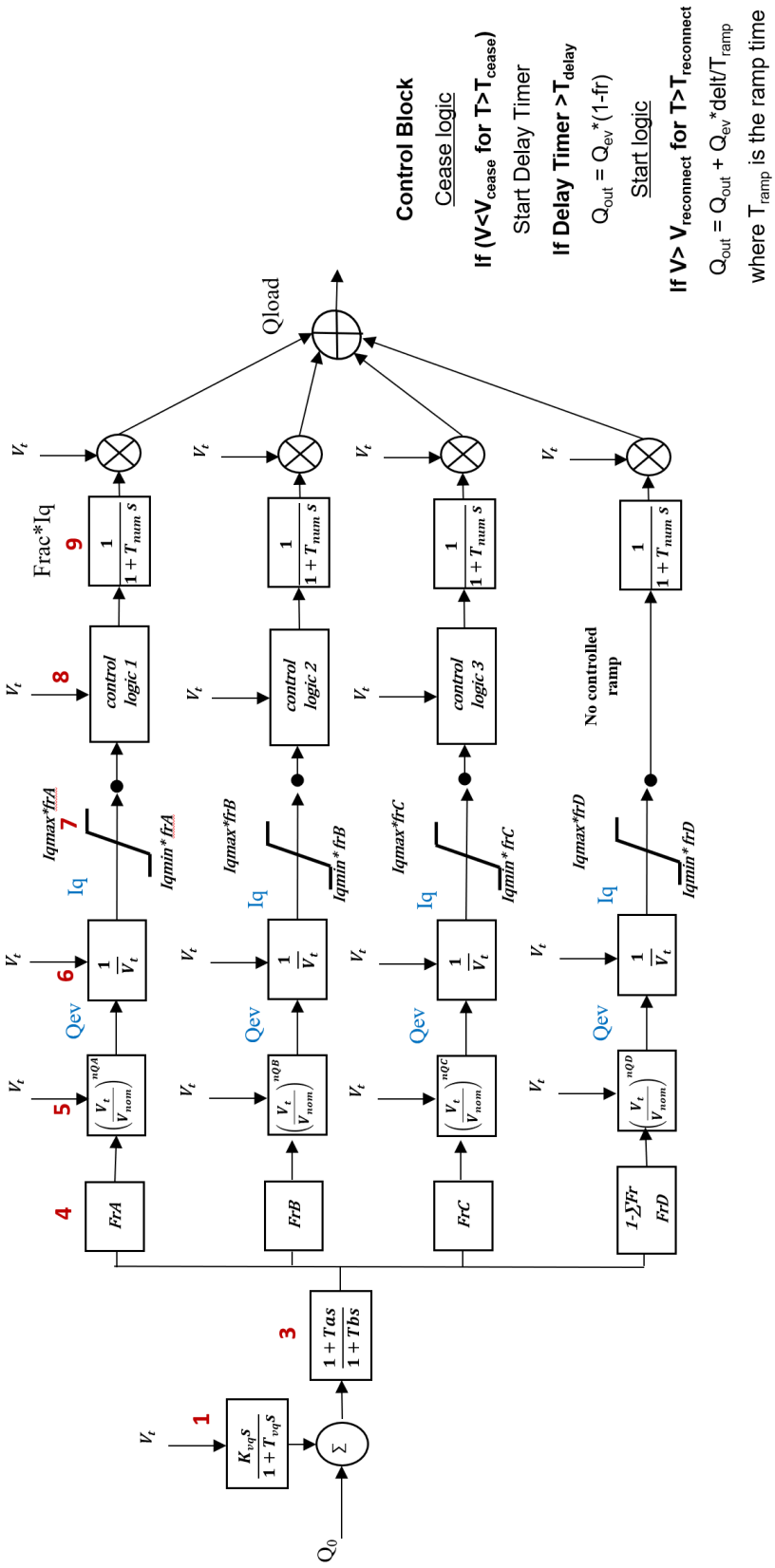

Figure 3 Reactive power control loop

The parameter/variable list and typical values for this model is tabulated in Table 1.

Table 1 Parameter list of EV charger model

Parameter	Parameter Description	Suggested Default
Tr	Voltage measurement time constant (s)	0.02
kdroop	Frequency droop gain	0
deadband	Deadband on frequency response	999
Kvp	Active power washout (Proportional constant)	0.2
Tvp	Active power washout (Time constant) (s)	0.02
Kvq	Reactive power washout (Proportional constant)	0.16
Tvq	Reactive power washout (Time constant) (s)	0.02
Ta	Lead time constant (s)	0.5
Tb	Lag time constant (s)	0.1
FrA	Fraction of Type A Evs	0.2
FrB	Fraction of Type B Evs	0.2
FrC	Fraction of Type C Evs	0.2
nPA	Active Power Exponential (FrA)	0
nQA	Reactive Power Exponential (FrA)	1
nPB	Active Power Exponential (FrB)	0
nQB	Reactive Power Exponential (FrB)	1
nPC	Active Power Exponential (FrC)	0
nQC	Reactive Power Exponential (FrC)	1
nPD	Active Power Exponential (FrD)	0

nQD	Reactive Power Exponential (FrD)	1
fcA	fraction of EV that will cease (FrA)	1
vcA	Voltage threshold for cease logic (FrA) (pu)	0.5
tcA	Time delay for cease logic to be initiated (FrA) (s)	0.01
tdelayA	Time delay to cease after detection (FrA) (s)	0.0
vrA	Voltage threshold to initiate power ramp logic (FrA) (pu)	0.6
trA	Time delay for ramp up logic to be initiated (FrA) (s)	0.05
trampA	Ramp up time (FrA) (s)	1
fcB	fraction of EV that will cease (FrB)	1
vcB	Voltage threshold for cease logic (FrB) (pu)	0.5
tcB	Time delay for cease logic to be initiated (FrB) (s)	0.01
tdelayB	Time delay to cease after detection (FrB) (s)	0.0
vrB	Voltage threshold to initiate ramp logic (FrB) (pu)	0.6
trB	Time delay for ramp up logic to be initiated (FrB) (s)	0.05
trampB	Ramp up time (FrB) (s)	1
fcC	fraction of EV that will cease (FrC)	1
vcC	Voltage threshold for cease logic (FrC) (pu)	0.5
tcC	Time delay for cease logic to be initiated (FrC) (s)	0.01
tdelayC	Time delay to cease after detection (FrC) (s)	0.0
vrC	Voltage threshold to initiate ramp logic (FrC) (pu)	0.6

trC	Time delay for ramp up logic to be initiated (FrC) (s)	0.05
trampC	Ramp up time (FrC) (s)	1
ipmin	minimum Ip (pu)	0
ipmax	maximum Ip (pu)	1.0
iqmin	minimum Iq (pu)	0
iqmax	maximum Iq (pu)	0.66

The output variables of the model are listed in Table

Table 2 Output variable list of EV charger model

Output Variable Name	Description
Pout	Cumulative Active Power Output (MW)
Qout	Cumulative Reactive Power Output (Mvar)
PfrA	Fraction A Active Power Output (MW)
QfrA	Fraction A Reactive Power Output (Mvar)
PfrB	Fraction B Active Power Output (MW)
QfrB	Fraction B Reactive Power Output (Mvar)
PfrC	Fraction C Active Power Output (MW)
QfrC	Fraction C Reactive Power Output (Mvar)
PfrD	Fraction D Active Power Output (MW)
QfrD	Fraction D Reactive Power Output (Mvar)
IPfA	Fraction A Active Current Component (pu)
IQfA	Fraction A Reactive Current Component (pu)
IPfB	Fraction B Active Current Component (pu)

IQfB	Fraction B Reactive Current Component (pu)
IPfC	Fraction C Active Current Component (pu)
IQfr	Fraction C Reactive current Component (pu)
IPfD	Fraction D Active Current Component (pu)
IQfD	Fraction D Reactive Current Component (pu)
FRA	Portion of Fraction A that did not cease
FRB	Portion of Fraction B that did not cease
FRC	Portion of Fraction C that did not cease
Vmea	Measured voltage (pu)

Simulation Results

Single Bus System

The first set of simulation is conducted using the GE PSLF™ simulator with a simple setup shown in Fig. 4 to test the dynamic performance of the EV charger model. The EV charger model is parameterized to replicate the response shown in Fig 1 and the parameters are given in Appendix A. The total active power consumed by this EV charger model is 21 kW. The active power load of individual fractions A, B, C, D are 3.2, 3.8, 3.6, and 10.4 kW respectively. Here, the play in voltage is the single source and so the response observed is that of the EV charger model alone. The same tests conducted in [4] (see Fig 1) is reproduced by reducing the voltage at terminal to 50% for 9 cycles as shown in Fig. 5. The response of each of the fractions is shown in Fig. 6, Fig. 7, Fig. 8 and Fig. 9. Note that, the plots on the left in each of the figures are the zoomed in sections near the fault for the plots on the right.

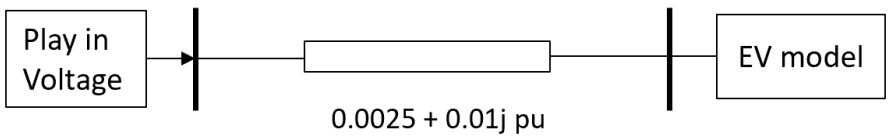

Figure 4 Single bus test system

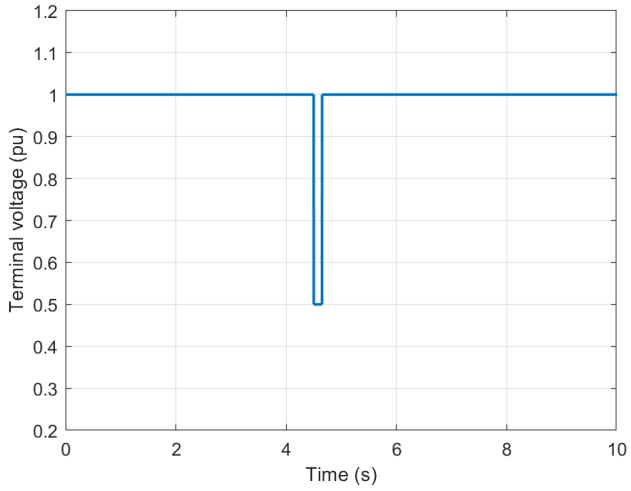

Figure 5 Voltage sag plot at the terminal of the load

- Fraction A replicates the behavior exhibited by EV-B chargers. The load reduces to zero (stops charging) right after the voltage drops and remains zero till about 13s as shown in Fig. 6. It then ramps up to the pre fault levels by 17.5s as shown in Fig. 6.
- Fraction B is used to represent EV-D type chargers that decreased their power consumption during the fault before reducing to zero after a time delay as shown in Fig. 7. Similar to the previous case, the active power is ramped after a set time delay of 8s.
- Fraction C response replicated EV-F type and is similar to Fraction A with smaller value of restart time and a faster ramp rate as shown in Fig. 8.
- EV chargers (EV-A, EV-C, EV-E) that behaved similar to a constant power load were modeled using the last fraction. Their response during voltage sag event is shown in Fig. 9. Please note there are small spikes in the active power output right after the fault is initiated and once when the fault is cleared. This is due to the delay introduced due to the numerical low pass filter.

The cumulative response is shown in Fig. 10. The dynamic model with parameters is included in the Appendix. A

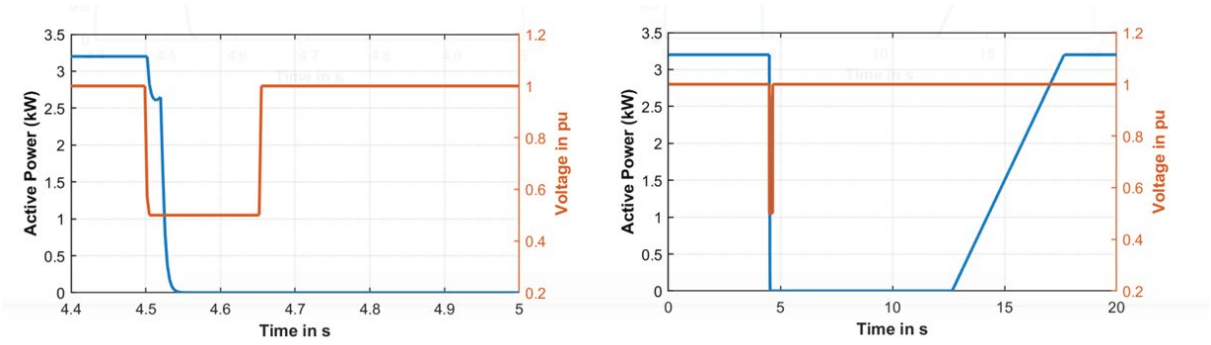

Figure 6 Response of fraction A of EV charger to the fault (EV-B)

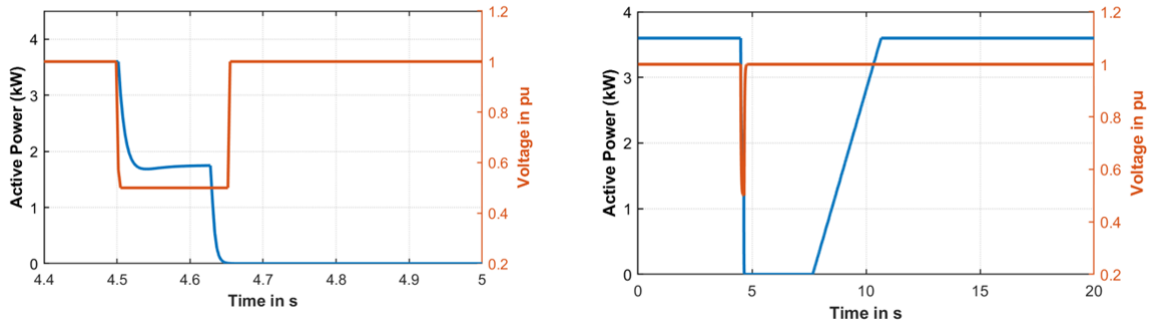

Figure 7 Response of fraction B of EV charger to the fault (EV-D)

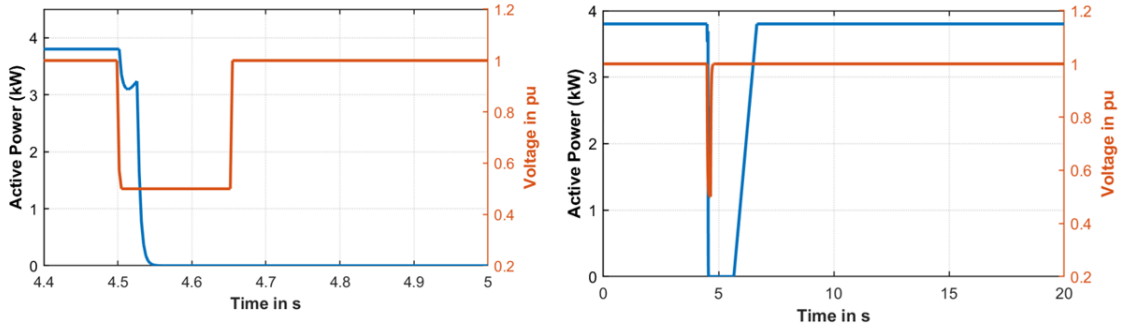

Figure 8 Response of fraction C of EV charger to the fault (EV-F)

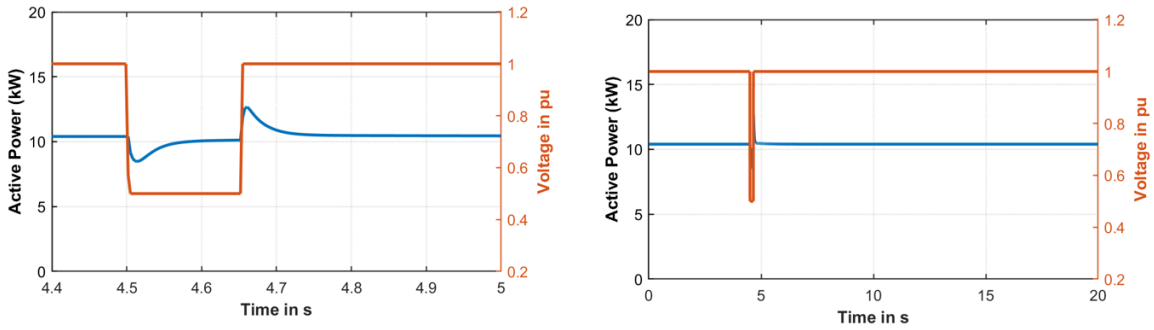

Figure 9 Response of last fraction of EV charger to the fault (EV-A, EV-C, EV-E)

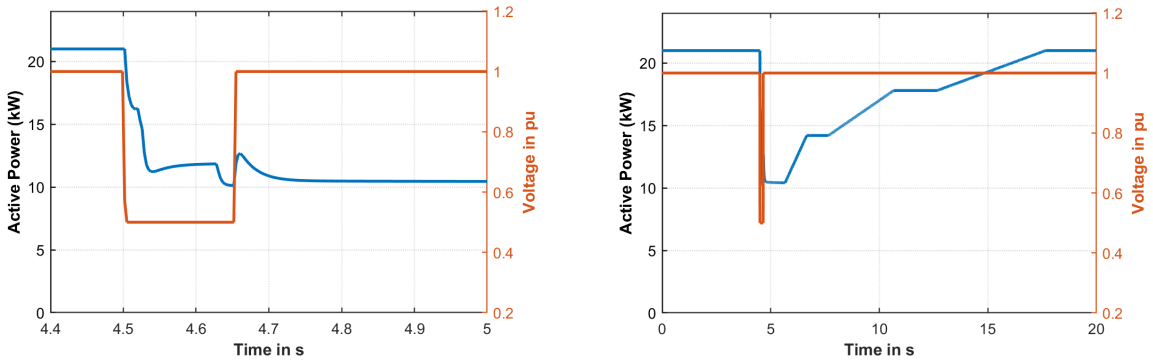

Figure 10 Cumulative response of the EV charger model to the fault

Key observations

- No numerical instability was observed due to the EV dynamic models during the simulation
- A single model EV charger model can replicate multiple distinct responses measured during experimentation and thus can be used to model aggregate response of EV chargers.

Another simulation study was done with the washout block disabled to check the numerical stability of the model. The response of each of the fractions is shown in Fig. 11, Fig. 12, Fig. 13, and Fig. 14 and their cumulative response is shown in Fig. 15. The simulation was stable and no significant change in response was noticed.

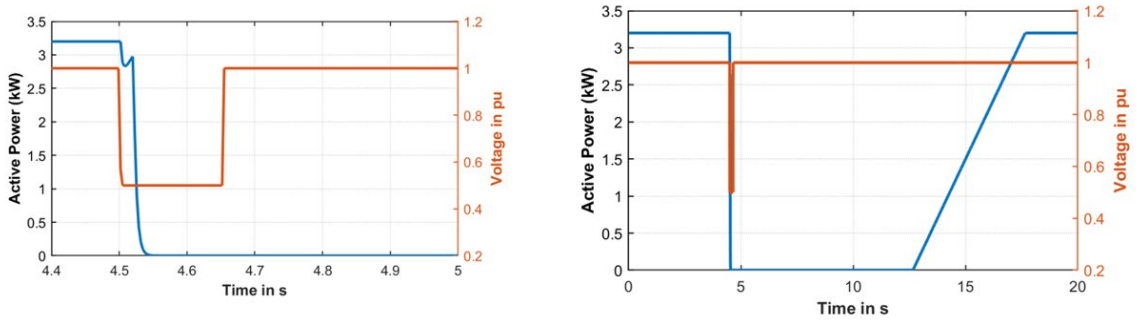

Figure 11 Response of fraction A of EV charger to the fault (Washout block disabled)

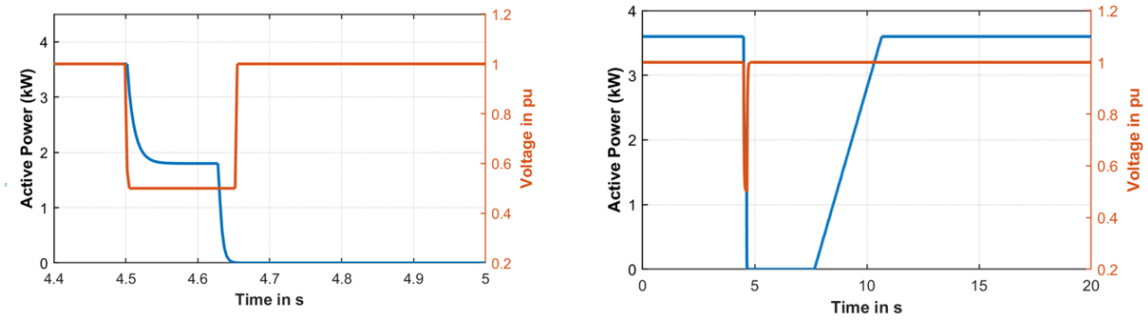

Figure 12 Response of fraction B of EV charger to the fault (Washout block disabled)

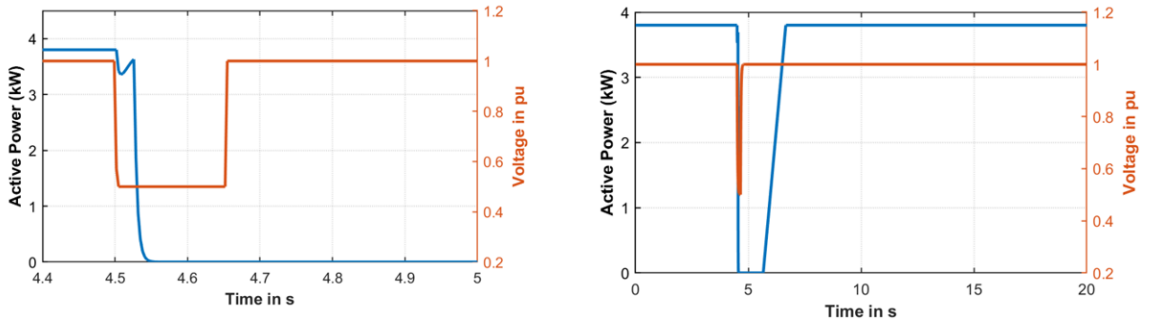

Figure 13 Response of fraction C of EV charger to the fault (Washout block disabled)

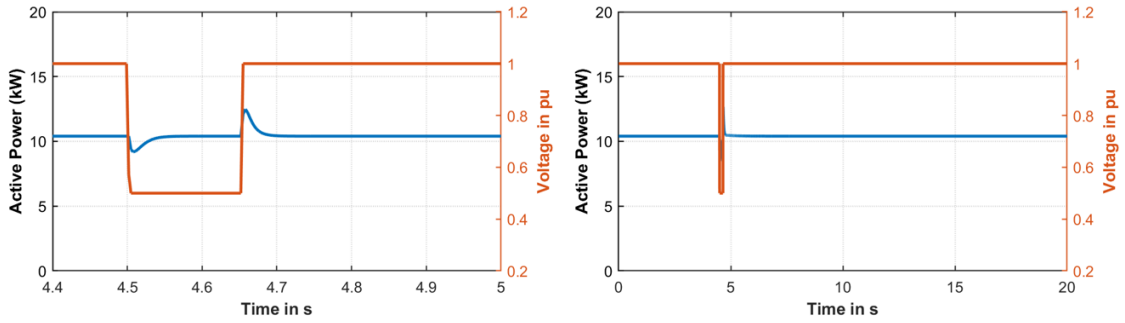

Figure 14 Response of last fraction of EV charger to the fault (Washout block disabled)

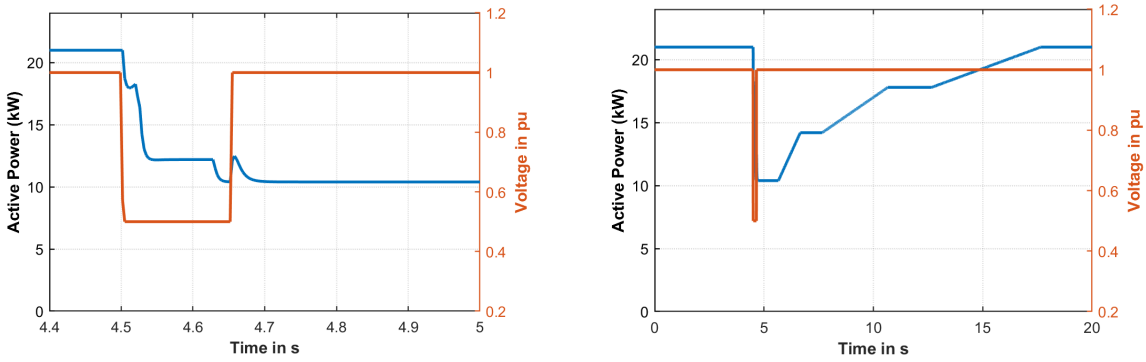

Figure 15 Cumulative response of the EV charger model to the fault (Washout block disabled)

22500 Bus System

The single bus system demonstrated capability of the EV charger model. In this section the scalability of the model for use in a practical transmission planning study and its numerical stability has been tested.

Simulation studies were conducted on a test system comparable to the size of the WECC system using the GE PSLF™ simulator. The test system contains 22500 buses and 3110 generators, 6410 instances of composite load models are present and account for 132 GW of total load.

For creating Scenario:

- Commercial and mixed feeder type buses with CMLD load in select zones were identified to incorporate EV charger models
- A new load was added in the power flow file to these buses to represent the EV charger loads
- The entire motor A load fraction and 50% of existing electronic load of CMLD was transferred to the new load ensuring that the total magnitude of the two loads on the bus was unchanged from the base case (this was done to create a portion of EV load and has no other meaning. The same could be done by reducing any other load component)
- The fraction of motor B, C, D was changed in the CMLD model accordingly so that the magnitude of each of these portions remained unchanged from the base case
- 1160 instances of EV charger load models were included for the simulation.
- Uniform parameters specified in Appendix A were used for all the EV charger load models.

Single Line to ground fault was applied at 345 kV line and cleared after 6 cycles and the response of the EV charger models at 40 buses is shown in Fig. 16.

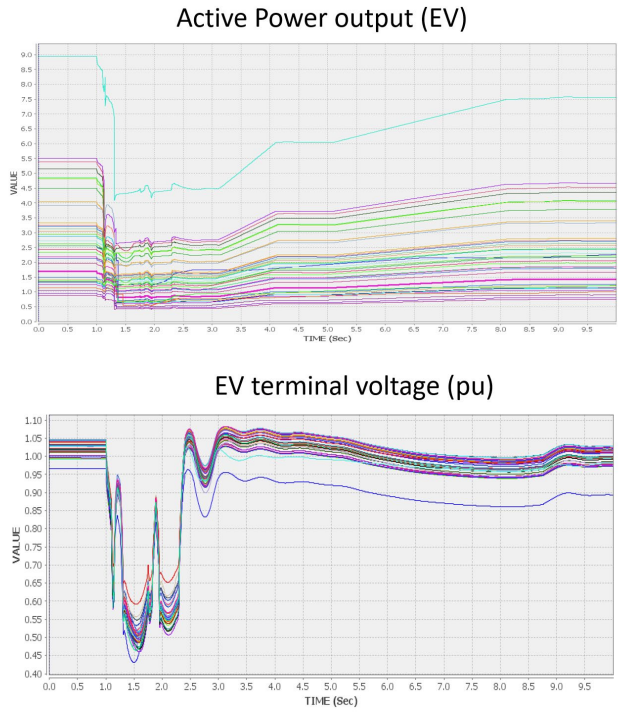

Figure 16 Response of the EV after a fault

Key observations

- No numerical instability was observed due to the EV dynamic models during the simulation
- 40 EV models were affected by the low voltage and the output of the EV ceased and ramped based on the parameters

Summary

A positive sequence model for simulating the aggregate behavior of EV chargers in dynamic response studies was developed in the PSLF simulator platform. The capability of the model to replicate distinct behavior observed in EV chargers was verified using a single bus test system. Furthermore, the numerical robustness and scalability of the model was verified using a 22500-bus test system.

References

[1] Technical update on load modeling'. Technical Report 3002013562, EPRI, Palo Alto, CA, 2018

[2] Jenn A, Highleyman J. Distribution grid impacts of electric vehicles: A California case study. iScience. 2021 Dec 28;25(1):103686. doi: 10.1016/j.isci.2021.103686. PMID: 35036872; PMCID: PMC8749456.

[3] "Simplified Model of PEV Charging During a Voltage Sag." Idaho National Laboratory as document number INL/EXT-19-55665

[4] Tuffner, Francis K., Undrill, John, Scoffield, Don, Eto, Joseph H., Kosterev, Dmitry, and Quint, Ryan D. Distribution-Level Impacts of Plug-in Electric Vehicle Charging on the Transmission System during Fault Conditions. United States: N. p., 2021. Web. doi:10.2172/1832905.

A
EXAMPLE DYNAMIC RECORD FOR PSLF FILE

epcmod 2 "Bus2 " 69.0 "1 " : #21 "EV_Chrg.p" 7.0 "Tr" 0.02 "Kvp" 0.20 "deadband" 0.017 "kdroop" 0 "Tvp" 0.02 "Kvq" 0.16 "Tvq" 0.02 "Ta" 0.1 "Tb" 0.2 "FrA" 0.1524 "FrB" 0.1714 "FrC" 0.1810 "nPA" 0.0 "nQA" 0.0 "nPB" 1.0 "nQB" 1.0 "nPC" 0.0 "nQC" 0.0 "nPD" 0.0 "nQD" 0.0 "fcA" 1.0 "vcA" 0.6 "tcA" 0.005 "tdelayA" 0.005 "vrA" 0.6 "trA" 8.0 "trampA" 5.0 "fcB" 1.0 "vcB" 0.7 "tcB" 0.12 "tdelayB" 0.005 "vrB" 0.6 "trB" 3.0 "trampB" 3.0 "fcC" 1.0 "vcC" 0.6 "tcC" 0.01 "tdelayC" 0.005 "vrC" 0.6 "trC" 1.0 "trampC" 1.0 "ipmax" 2.0 "ipmin" -2.0 "iqmax" 2.0 "iqmin" -2.0

Note: **EPCL model EV_Chrg.p is available as a separate attachment**.

Export Control Restrictions

Access to and use of this EPRI product is granted with the specific understanding and requirement that responsibility for ensuring full compliance with all applicable U.S. and foreign export laws and regulations is being undertaken by you and your company. This includes an obligation to ensure that any individual receiving access hereunder who is not a U.S. citizen or U.S. permanent resident is permitted access under applicable U.S. and foreign export laws and regulations.

In the event you are uncertain whether you or your company may lawfully obtain access to this EPRI product, you acknowledge that it is your obligation to consult with your company's legal counsel to determine whether this access is lawful. Although EPRI may make available on a case by case basis an informal assessment of the applicable U.S. export classification for specific EPRI products, you and your company acknowledge that this assessment is solely for informational purposes and not for reliance purposes.

Your obligations regarding U.S. export control requirements apply during and after you and your company's engagement with EPRI. To be clear, the obligations continue after your retirement or other departure from your company, and include any knowledge retained after gaining access to EPRI products.

You and your company understand and acknowledge your obligations to make a prompt report to EPRI and the appropriate authorities regarding any access to or use of this EPRI product hereunder that may be in violation of applicable U.S. or foreign export laws or regulations.

About EPRI

Founded in 1972, EPRI is the world's preeminent independent, non-profit energy research and development organization, with offices around the world. EPRI's trusted experts collaborate with more than 450 companies in 45 countries, driving innovation to ensure the public has clean, safe, reliable, affordable, and equitable access to electricity across the globe. Together, we are shaping the future of energy.

3002xxxxxx

EPRI
3420 Hillview Avenue, Palo Alto, California 94304-1338 • USA
800.313.3774 • 650.855.2121 • askepri@epri.com • www.epri.com